



Effect of cobalt content on the properties of quintuple perovskites $\text{Sm}_2\text{Ba}_3\text{Fe}_{5-x}\text{Co}_x\text{O}_{15-\delta}$

I.B. Golovachev^a, M. Yu. Mychinko^b, N.E. Volkova^{a,*}, L. Ya. Gavrilova^a, B. Raveau^c,
A. Maignan^{a,c}, V.A. Cherepanov^a

^a Institute of Natural Science and Mathematics, Ural Federal University, Lenin Av., 51, Yekaterinburg, 620000, Russia

^b Electron Microscopy for Materials Science (EMAT), University of Antwerp, Groenenborgerlaan 171, 2020, Antwerp, Belgium

^c Laboratoire CRISMAT, UMR 6508 Normandie Université, CNRS, ENSICAEN, UNICAEN, 6 bd du Maréchal Juin, 14050, CAEN Cedex 4, France



ARTICLE INFO

Keywords:

Multilayer structure
Semiconductors
Electrical properties
Thermal properties

ABSTRACT

Quintuple perovskites $\text{Sm}_2\text{Ba}_3\text{Fe}_{5-x}\text{Co}_x\text{O}_{15-\delta}$ ($x = 0.5, 1.0$ and 1.5) have been prepared by glycerin-nitrate technique in air. The phase purity was confirmed by XRD. Partial substitution of Co for Fe decreases the oxygen content and thus the mean oxidation state of 3d-metals. It also slightly decreases the thermal expansion coefficient of oxides. Positive value of the Seebeck coefficient confirmed *p*-type conductivity, though the thermopower decreases as the Co content increases. The temperature dependence of electrical conductivity reveals a maximum at 550–750 °C.

1. Introduction

Layered perovskites are considered as promising cathode materials for intermediate-temperature solid oxide fuel cell (IT-SOFC) because of their superior mixed electronic-ionic conduction properties and high thermal stability [1–11].

Recently a new class of 5-fold layered nanoscale-ordered $\text{Ln}_{2-\varepsilon}\text{Ba}_{3+\varepsilon}\text{Fe}_5\text{O}_{15-\delta}$ oxides was detected in the $\text{Ln}_2\text{O}_3 - \text{BaO} - \text{Fe}_2\text{O}_3$ ($\text{Ln} = \text{Nd}, \text{Sm}, \text{Eu}, \text{Gd}$) systems in air [12–16]. This 5-fold layered structure is formed by alternation of the layers containing exclusively lanthanide or barium together with the mixed (Ln,Ba) layers along the *c*-axis in a sequence: Ln-Ba-(Ln,Ba)-(Ln,Ba)-Ba-Ln. The oxygen content, which is closely related with oxidation state of 3d metals, plays an important role in formation of quintuple perovskite superstructure. In Co-free samarium barium ferrite the required oxygen content in air condition can be achieved only by means of partial substitution (ε) of Ba for Sm forming $\text{Ln}_{2-\varepsilon}\text{Ba}_{3+\varepsilon}\text{Fe}_5\text{O}_{15-\delta}$ with $\varepsilon = 0.125$. Here barium serves as an acceptor-type dopant Ba'_{Sm} located in a mixed (Ln/Ba) layer and thus allow decreasing the value of oxygen content (raise oxygen vacancy concentration $[V_{\text{O}}]$). Partial substitution of Co for Fe makes unnecessary stoichiometry deviation in A-site sublattice ($\varepsilon = 0$) since in this case cobalt ions serve as acceptor-type substituent Co'_{Fe} and allow to decrease oxygen content in $\text{Sm}_2\text{Ba}_3\text{Fe}_{5-x}\text{Co}_x\text{O}_{15-\delta}$ down to its favorable value [13–16].

The aforementioned complex layered structure was also attracting attention in terms of practical application. Co-free quintuple perovskite $\text{Sm}_{1.875}\text{Ba}_{3.125}\text{Fe}_5\text{O}_{15-\delta}$ was recently considered as a novel cathode for IT-SOFCs [17].

Since both oxygen content and substitution of Co for Fe govern the formation of 5-fold layered superstructure, in this paper we examined the effect of Co introduction on oxygen content, electrical properties and thermal expansion of $\text{Sm}_2\text{Ba}_3\text{Fe}_{5-x}\text{Co}_x\text{O}_{15-\delta}$ ($x = 0.5-1.5$) solid solutions.

2. Material and methods

The samples of $\text{Sm}_2\text{Ba}_3\text{Fe}_{5-x}\text{Co}_x\text{O}_{15-\delta}$ ($x = 0.5, 1.0$ and 1.5) were prepared using a glycerin nitrate technique using high-purity Sm_2O_3 , BaCO_3 , $\text{FeC}_2\text{O}_4 \times 2\text{H}_2\text{O}$, Co, HNO_3 and glycerol as starting materials. The starting reagents weighted in the required amounts were dissolved in nitric acid, and then glycerol was added to the solution. Further details of glycerol-nitrate technique were described earlier elsewhere [16]. Final anneals were performed at 1100 °C in air for 120 h employing several steps (≈ 20 h each) and intermediate grinding. Finally, samples were slowly cooled to room temperature at a rate of about 70 °C/h. The phase composition of the annealed samples was determined by X-ray diffraction (XRD) using a Shimadzu XRD-7000 instrument (CuK α -radiation, angle range $2\theta = 20^\circ-90^\circ$, step 0.02° , 5 s/step) in air. The structural parameters were refined by the Le-Bail method using the Fullprof-2008

* Corresponding author.

E-mail address: nadezhda.volkova@urfu.ru (N.E. Volkova).

<https://doi.org/10.1016/j.jssc.2021.122324>

Received 6 April 2021; Received in revised form 31 May 2021; Accepted 1 June 2021

Available online 3 June 2021

0022-4596/© 2021 Elsevier Inc. All rights reserved.

package. Thermogravimetric analysis (TGA) was carried out using a STA 409PC instrument (Netzsch) within the temperature range 25–1100 °C in air in dynamic (heating/cooling rate 5 °C/min) mode and static mode (isothermal exposure for 8 h). The absolute values of oxygen content in the samples at room temperature were taken from ref [16]. Thermal expansion of ceramic samples was measured using a high temperature dilatometer DIL 402 C (Netzsch) in the temperature range 25–1100 °C in air with a heating/cooling rate of 5 °C/min. Total electrical conductivity (σ) and the Seebeck coefficient (S) of ceramic samples were measured by a standard 4-probe DC method with platinum electrodes within the temperature range 25–1100 °C. Temperature and P_{O_2} control, as well as, data collection were performed with a Zirconia 318 instrument [18]. Dense ceramic samples in the form of bars ($3 \times 3 \times 25 \text{ mm}^3$) for dilatometry and electrical properties measurements were prepared by uniaxial pressing of the powders under pressure of 20 bar, followed by sintering at 1300–1350 °C for 12 h. The samples were slowly cooled to room temperature at a rate of 50 °C/h. The density of the samples was calculated as the quotient of dividing the mass by the volume obtained from the geometric dimensions of the ceramic bars. The densities of the polished ceramic samples were 92–95% of the theoretical value calculated from the XRD data.

3. Results and discussion

It was shown already by HRTEM that all $\text{Sm}_2\text{Ba}_3\text{Fe}_{5-x}\text{Co}_x\text{O}_{15-\delta}$ ($x = 0.5\text{--}1.5$) oxides possess 5-fold tetragonal $a_p \times a_p \times 5a_p$ superstructure [16]. Although XRD analysis cannot detect the formation of a layered ordered supercell due to chemical twinning along the orthogonal directions [12–16] it can confirm single phase purity. Accordingly, the XRD results of all obtained samples were single-phase that can be described in terms of the cubic perovskite structure (SG $Pm\bar{3}m$). The XRD patterns for the single-phase $\text{Sm}_2\text{Ba}_3\text{Fe}_{5-x}\text{Co}_x\text{O}_{15-\delta}$ refined by the Le-Bail method are presented in supplementary (Fig. S1). The refined unit cell parameters were found to be in good agreement with those reported in Ref. [16]. No traces of starting materials or secondary phase were detected.

Fig. 1 illustrates the variation of oxygen content in $\text{Sm}_2\text{Ba}_3\text{Fe}_{5-x}\text{Co}_x\text{O}_{15-\delta}$ as a function of temperature in air. The oxygen content and average oxidation state of 3d-metal ions (z_{Me}) in the $\text{Sm}_2\text{Ba}_3\text{Fe}_{5-x}\text{Co}_x\text{O}_{15-\delta}$ oxides, either slowly cooled to room temperature or those related to 1100 °C (taken from TGA measurements) are listed in Table 1.

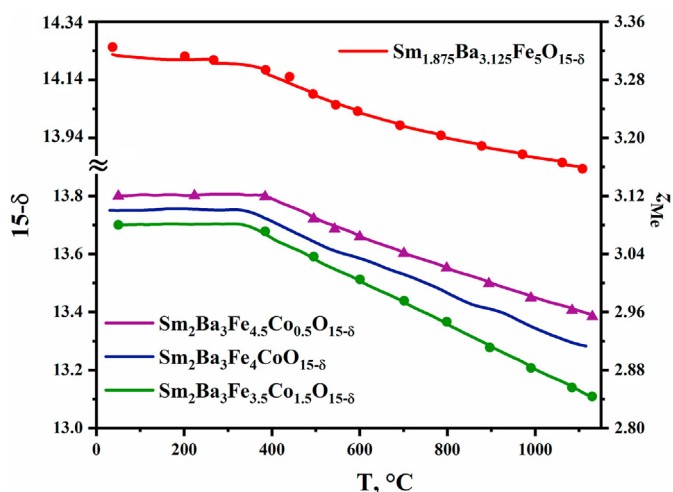


Fig. 1. Oxygen content and mean oxidation state of 3 d metals in $\text{Sm}_2\text{Ba}_3\text{Fe}_{5-x}\text{Co}_x\text{O}_{15-\delta}$ at $P_{O_2} = 0.21 \text{ atm}$. Solid lines represent data obtained in dynamic mode measurements (cooling/heating rate of 5 °C/min), and points correspond to the values measured in static mode (isothermal dwells for 8 h). The plot for Co-free sample (upper red line) was calculated using values of oxygen content presented in Ref. [12]. (For interpretation of the references to colour in this figure legend, the reader is referred to the web version of this article.)

Table 1

Oxygen content ($15-\delta$), mean oxidation state of 3d metal ions (z_{Me}) in $\text{Sm}_2\text{Ba}_3\text{Fe}_{5-x}\text{Co}_x\text{O}_{15-\delta}$ at 25 and 1100 °C together with average thermal expansion coefficients (TECs) calculated from the dilatometry at 1000 °C.

Composition	15- δ (25 °C) recalculated from [16]	z_{Me} (25 °C) [16]	15- δ (1100 °C)	z_{Me} (1100 °C)	TEC $\times 10^6$, K^{-1}
$\text{Sm}_2\text{Ba}_3\text{Fe}_{4.5}\text{Co}_{0.5}\text{O}_{15-\delta}$	13.80 ± 0.2	3.12	13.40 ± 0.2	2.96	–
$\text{Sm}_2\text{Ba}_3\text{Fe}_4\text{CoO}_{15-\delta}$	13.75 ± 0.2	3.10	13.29 ± 0.2	2.92	17.8
$\text{Sm}_2\text{Ba}_3\text{Fe}_{3.5}\text{Co}_{1.5}\text{O}_{15-\delta}$	13.70 ± 0.2	3.08	13.13 ± 0.2	2.85	17.2

The values of oxygen content and mean oxidation state of 3d metal ions (see Fig. 1) are decreasing with the raise of cobalt concentration in $\text{Sm}_2\text{Ba}_3\text{Fe}_{5-x}\text{Co}_x\text{O}_{15-\delta}$ within the entire temperature range. The amount of oxygen losses while heating from room temperature up to 1100 °C ($\Delta\delta = \delta_{1100^\circ\text{C}} - \delta_{25^\circ\text{C}}$) also gradually increases with Co content. These trends can be explained in terms of binding energy between 3d-metal and oxygen, which is smaller for Co in comparison with Fe ions ($\Delta H^\circ_{\text{Fe-O}} = 409(13) \text{ kJ/mol}$, $\Delta H^\circ_{\text{Co-O}} = 368(21) \text{ kJ/mol}$) [19].

Partial substitution of Co for Fe makes decreasing the slope of thermal expansion versus temperature for $\text{Sm}_2\text{Ba}_3\text{Fe}_{5-x}\text{Co}_x\text{O}_{15-\delta}$ ($x = 1; 1.5$) compared to Co-free sample (Fig. 2). Excellent reproducibility and absence of hysteresis between the dilatometric data collected on heating and cooling, indicate high rate of oxygen exchange and confirm absence of phase transition within the temperature range studied. The average thermal expansion coefficients (TECs) calculated from the dilatometry are listed in Table 1.

The temperature dependencies of total conductivity and Seebeck coefficient for $\text{Sm}_2\text{Ba}_3\text{Fe}_{5-x}\text{Co}_x\text{O}_{15-\delta}$ in air are shown in Fig. 3a and b.

Since introduction of Co decreasing the slope of relative linear expansion versus temperature, the conductivity value for the sample with cobalt content $y = 1.0$ is close to that for the Co-free sample, and the sample with $y = 1.5$ showed increased conductivity, we decided not to measure the physical properties of the sample with the smallest Co content $y = 0.5$.

The positive value of Seebeck coefficient (Fig. 3b) indicates predominant p-type conductivity in $\text{Sm}_2\text{Ba}_3\text{Fe}_{5-x}\text{Co}_x\text{O}_{15-\delta}$. Interestingly that conductivity of the sample with $x = 1$ at $T > 400^\circ\text{C}$ is close to Co-free oxide while the value for $\text{Sm}_2\text{Ba}_3\text{Fe}_{3.5}\text{Co}_{1.5}\text{O}_{15-\delta}$ is noticeably higher (Fig. 3a). It can be seen in the inset of Fig. 1 that the mean oxidation state of 3d-metal is greater than 3 ($z_{Me} > 3$) in $\text{Sm}_{1.875}\text{Ba}_{3.125}\text{Fe}_5\text{O}_{15-\delta}$ within

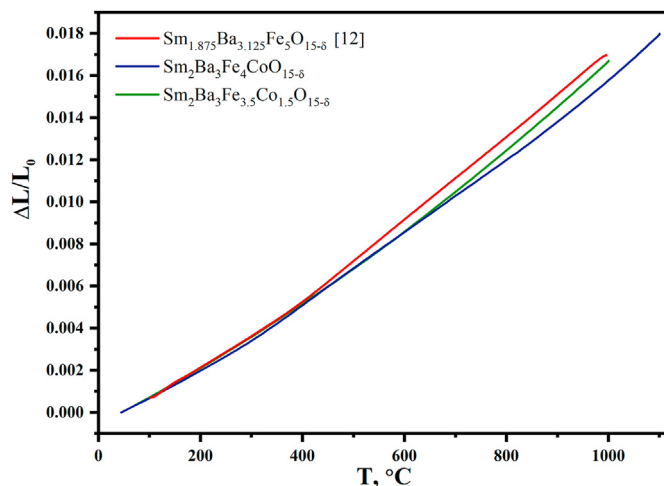


Fig. 2. Thermal expansion of the $\text{Sm}_2\text{Ba}_3\text{Fe}_{5-x}\text{Co}_x\text{O}_{15-\delta}$ ceramics in air in comparison with data for $\text{Sm}_{1.875}\text{Ba}_{3.125}\text{Fe}_5\text{O}_{15-\delta}$ [12].

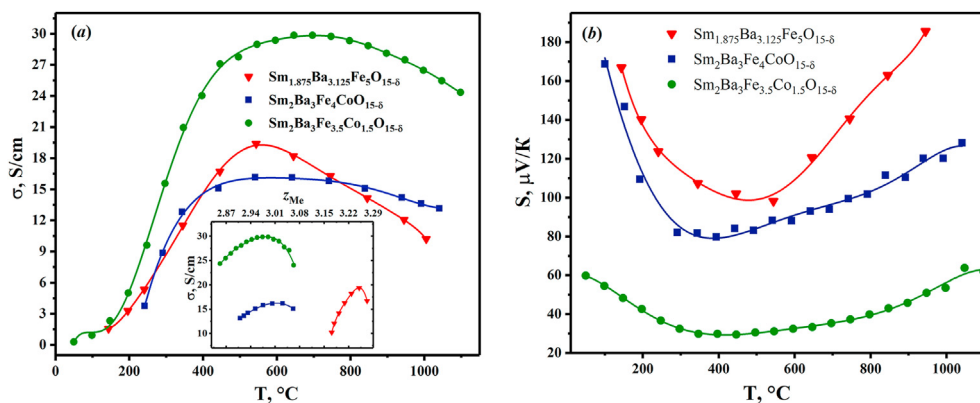


Fig. 3. Temperature dependencies of total conductivity (a) and Seebeck coefficient (b) for $\text{Sm}_{2-\epsilon}\text{Ba}_{3+\epsilon}\text{Fe}_{5-x}\text{Co}_x\text{O}_{15-\delta}$ in air. Inset in Fig. 3 (a) shows conductivity versus mean oxidation state of 3d metals. The values of conductivity for the Co-free sample are taken from Ref. [12].

entire temperature range, while in Co-doped oxides ($x = 1.0$ and 1.5) its value is much smaller. This means that concentration of mobile holes according to a simple electroneutrality approach should be higher in the Co-free sample.

Moreover, $z_{\text{Me}} < 3$ in Co-doped oxides at $T > 630^\circ\text{C}$ for $x = 1$ and $T > 530^\circ\text{C}$ for $x = 1.5$, therefore electronic holes can appear only by means of the intrinsic charge disproportionation process:



Indeed, such temperature activated disproportionation is well acknowledged in rare earth cobaltites and ferrites with perovskite structure [20–24].

Simultaneous presence of Fe and Co in B-sublattice makes such electronic disordering exchange process even more pronounced:



since Co as more electronegative elements serves as acceptor-type substituent.

Predominant coexistence of $\text{Fe}^{3+}/\text{Fe}^{4+}$ ions in the studied Co-free oxide and related perovskite materials [25] allow to neglect disproportionation of Fe^{3+} . Thus, although on the one hand the raise of Co content results in decreasing oxygen content, and therefore the value of z_{Me} (see inset in Fig. 3a), on the other hand it enhances electronic exchange process (2) and therefore increases charge carrier concentration. This peculiar role of trivalent cobalt is consistent with the sign of the Seebeck coefficient being either positive or negative depending on doping in LaCoO_3 [26].

The raise of total conductivity with temperature up to a maximum value at $T \approx 550\text{--}750^\circ\text{C}$ can be explained by the increase of mobility and concentration of electronic holes that appear according to equation (1). At higher temperatures ($T > 600^\circ\text{C}$), the total conductivity slightly decreases that caused by an increase in oxygen deficiency, which is preventing formation of electron holes (M_{Fe}^{\bullet}) according to the reaction:



Similar temperature dependencies with a maximum were obtained for a number of related double perovskite materials [1, 5–7.9–11].

4. Conclusions

The $\text{Sm}_2\text{Ba}_3\text{Fe}_{5-x}\text{Co}_x\text{O}_{15-\delta}$ ($x = 0.5, 1.0$ and 1.5) oxides have been synthesized by the glycerin nitrate technique in air. Introduction of cobalt decreases the value of oxygen content as well as mean oxidation state of 3d metals and allows the formation of a single-phase 5-fold layered superstructure without Sm/Ba ratio shift comparing to ideal

stoichiometric composition. This Co-substitution slightly decreases TEC values. Electrical conductivity versus temperature of $\text{Sm}_2\text{Ba}_3\text{Fe}_{5-x}\text{Co}_x\text{O}_{15-\delta}$ exhibit maxima at relatively high temperature; this is explained by the progressive oxygen losses starting at high temperature. Interestingly, the first step of Co-substitution ($x = 1.0$) has not affected conductivity since two opposite factors, i.e. decrease in oxygen content and enhanced electronic exchange between Fe^{3+} and Co^{3+} ions, compensate each other. Further incorporation of Co ($x = 1.5$) facilitating the latter leads an increase of the conductivity.

CRediT authorship contribution statement

I.B. Golovachev: Investigation, Writing – original draft. **M. Yu. Mychinko:** Investigation, Formal analysis, Funding acquisition. **N.E. Volkova:** Investigation, Validation, Visualization. **L. Ya. Gavrilova:** Conceptualization, Methodology. **B. Raveau:** Writing – review & editing, Supervision. **A. Maignan:** Writing – review & editing, Supervision, Funding acquisition. **V.A. Cherepanov:** Conceptualization, Writing – review & editing, Supervision.

Declaration of competing interest

The authors declare that they have no known competing financial interests or personal relationships that could have appeared to influence the work reported in this paper.

Acknowledgement

The work was financially supported in parts from the Ministry of Science and Higher Education of Russian Federation [Agreement No. 075-15-2019-1924] and Russian Foundation for Basic Research [project No 18-33-00822].

Appendix A. Supplementary data

Supplementary data to this article can be found online at <https://doi.org/10.1016/j.jssc.2021.122324>.

References

- [1] A.K. Azad, J.H. Kim, J.T.S. Irvine, Structure–property relationship in layered perovskite cathode $\text{LnBa}_{0.5}\text{Sr}_{0.5}\text{Co}_2\text{O}_{5+\delta}$ ($\text{Ln}=\text{Pr},\text{Nd}$) for solid oxide fuel cells, *J. Power Sources* 196 (2011) 7333–7337, <https://doi.org/10.1016/j.jpowsour.2011.02.063>.
- [2] A. Chang, S.J. Skinner, J.A. Kilner, Electrical properties of $\text{GdBaCo}_2\text{O}_{5+x}$ for ITSOFC applications, *Solid State Ion* 177 (2006) 2009–2011, <https://doi.org/10.1016/j.ssi.2006.05.047>.
- [3] M.V. Ananyev, V.A. Eremin, D.S. Tsvetkov, N.M. Porotnikova, A.S. Farlenkov, A.Yu. Zuev, A.V. Fetisov, E.Kh. Kurumchin, Oxygen isotope exchange and diffusion

- in $\text{LnBaCo}_2\text{O}_{6-\delta}$ (Ln=Pr,Sm,Gd) with double perovskite structure, *Solid State Ion* 304 (2017) 96–106, <https://doi.org/10.1016/j.ssi.2017.03.022>.
- [4] Z. Du, K. Li, H. Zhao, X. Dong, Y. Zhanga, K. Świerczek, A. SmBaCo₂O_{5+δ} double perovskite with epitaxially grown Sm_{0.2}Ce_{0.8}O_{2-δ} nanoparticles as a promising cathode for solid oxide fuel cells, *J. Mater. Chem. A* 8 (2020) 14162–14170, <https://doi.org/10.1039/d0ta05602b>.
- [5] D. Chen, F. Wang, H. Shi, R. Ran, Z. Shao, Systematic evaluation of Co-free LnBaFe₂O_{5+δ} (Ln = Lanthanides or Y) oxides towards the application as cathodes for intermediate-temperature solid oxide fuel cells, *Electrochim. Acta* 78 (2012) 466–474, <https://doi.org/10.1016/j.electacta.2012.06.073>.
- [6] Z. He, L. Xia, Y. Chen, J. Yu, X. Huang, Y. Yu, Layered perovskite Sm_{1-x}La_xBaFe₂O_{5+δ} as cobalt-free cathodes for IT-SOFCs, *RSC Adv.* 5 (2015) 57592–57598, <https://doi.org/10.1039/c5ra09762b>.
- [7] F. Meng, T. Xia, J. Wang, Z. Shi, H. Zhao, Praseodymium-deficiency Pr_{0.94}BaCo₂O_{6-δ} double perovskite: a promising high performance cathode material for intermediate-temperature solid oxide fuel cells, *J. Power Sources* 293 (2015) 741–750, <https://doi.org/10.1016/j.jpowsour.2015.06.007>.
- [8] Y.N. Kim, J.H. Kim, A. Manthiram, Effect of Fe substitution on the structure and properties of LnBaCo_{2-x}Fe_xO_{5+δ} (Ln = Nd and Gd) cathodes, *J. Power Sources* 195 (2010) 6411–6419, <https://doi.org/10.1016/j.jpowsour.2010.03.100>.
- [9] F. Jin, H. Xu, W. Long, Y. Shen, T. He, Characterization and evaluation of double perovskites LnBaCoFeO_{5+δ} (Ln=Pr and Nd) as intermediate-temperature solid oxide fuel cell cathodes, *J. Power Sources* 243 (2013) 10–18, <https://doi.org/10.1016/j.jpowsour.2013.05.187>.
- [10] L. Zhao, J. Shen, B. He, F. Chen, C. Xia, Synthesis, characterization and evaluation of PrBaCo_{2-x}Fe_xO_{5+δ} as cathodes for intermediate-temperature solid oxide fuel cells, *Int. J. Hydrogen Energy* 36 (2011) 3658–3665, <https://doi.org/10.1016/j.ijhydene.2010.12.064>.
- [11] N.E. Volkova, L.Ya Gavrilova, V.A. Cherepanov, T.V. Aksenova, V.A. Kolotygin, V.V. Kharton, Synthesis, crystal structure and properties of SmBaCo_{2-x}Fe_xO_{5+δ}, *J. Solid State Chem.* 204 (2013) 219–223, <https://doi.org/10.1016/j.jssc.2013.06.001>.
- [12] N.E. Volkova, O.I. Lebedev, L.Ya Gavrilova, S. Turner, N. Gauquelin, Mdm. Seikh, V. Caignaert, V.A. Cherepanov, B. Raveau, G. Van Tendeloo, Nanoscale ordering in oxygen deficient quintuple perovskite Sm_{2-x}Ba_{3+x}Fe₅O_{15-δ}: implication for magnetism and oxygen stoichiometry, *Chem. Mater.* 26 (2014) 6303–6310, <https://doi.org/10.1021/cm503276p>.
- [13] A.K. Kundu, O.I. Lebedev, N.E. Volkova, Mdm. Seikh, V. Caignaert, V.A. Cherepanov, B. Raveau, Quintuple perovskites Ln₂Ba₃Fe_{5-x}Co_xO_{15-δ} (Ln=Sm,Eu): nanoscale ordering and unconventional magnetism, *J. Mater. Chem. C* 3 (2015) 5398–5405, <https://doi.org/10.1039/C5TC00494B>.
- [14] A.K. Kundu, M.Yu Mychinko, V. Caignaert, O.I. Lebedev, N.E. Volkova, K.M. Deryabina, V.A. Cherepanov, B. Raveau, Coherent intergrowth of simple cubic and quintuple tetragonal perovskites in the system Nd_{2-x}Ba_{3+x}(Fe,Co)₅O_{15-δ}, *J. Solid State Chem.* 231 (2015) 36–41, <https://doi.org/10.1016/j.jssc.2015.07.050>.
- [15] N.E. Volkova, A.S. Urusova, L.Ya Gavrilova, A.V. Bryuzgina, K.M. Deryabina, M.Yu Mychinko, O.I. Lebedev, B. Raveau, V.A. Cherepanov, Specific features of phase equilibria in Ln–Ba–Fe–O systems, *Russ. J. Gen. Chem.* 86 (2016) 1800–1804, <https://doi.org/10.1134/S1070363216080041>.
- [16] N.E. Volkova, M.Yu Mychinko, I.B. Golovachev, A.E. Makarova, M.V. Bazueva, E.I. Zyaikin, L.Ya Gavrilova, V.A. Cherepanov, Structure and properties of layered perovskites Ba_{1-x}Ln_xFe_{1-y}Co_yO_{3-δ} (Ln = Pr, Sm, Gd), *J. Alloys Compd.* 784 (2019) 1297–1302, <https://doi.org/10.1016/j.jallcom.2018.12.391>.
- [17] Q. Zhou, L. Chen, Y. Cheng, Y. Xie, Cobalt-free quintuple perovskite Sm_{1.875}Ba_{3.125}Fe₅O_{15-δ} as a novel cathode for intermediate temperature solid oxide fuel cells, *Ceram. Int.* 42 (2016) 10469–10471, <https://doi.org/10.1016/j.ceramint.2016.03.174>.
- [18] A.Yu Zuev, A.I. Vylkov, A.N. Petrov, D.S. Tsvetkov, Defect structure and defect-induced expansion of undoped oxygen deficient perovskite LaCoO_{3-δ}, *Solid State Ion* 179 (2008) 1876–1879, <https://doi.org/10.1016/j.ssi.2008.06.001>.
- [19] T.L. Cottrell, *The Strengths of Chemical Bonds*, Butterworth, London, 1958, p. 310.
- [20] E. Bucher, W. Sitte, Defect chemical analysis of the electronic conductivity of strontium-substituted lanthanum ferrite, *Solid State Ion* 173 (2004) 23–28, <https://doi.org/10.1016/j.ssi.2004.07.047>.
- [21] P.M. Raccach, J.B. Goodenough, A localized-electron collective-electron transition in the system (La,Sr)CoO, *J. Appl. Phys.* 39 (1968) 1209–1210, <https://doi.org/10.1063/1.1656227>.
- [22] J. Mizusaki, M. Yoshihiro, S. Yamauchi, K. Fueki, Nonstoichiometry and defect structure of the perovskite-type oxides La_{1-x}Sr_xFeO_{3-δ}, *J. Solid State Chem.* 58 (1985) 257–266, [https://doi.org/10.1016/0022-4596\(85\)90243-9](https://doi.org/10.1016/0022-4596(85)90243-9).
- [23] J. Mizusaki, Y. Mima, S. Yamauchi, K. Fueki, H. Tagawa, Nonstoichiometry of the perovskite-type oxide La_{1-x}Sr_xCoO_{3-δ}, *J. Solid State Chem.* 80 (1989) 102–111, [https://doi.org/10.1016/0022-4596\(89\)90036-4](https://doi.org/10.1016/0022-4596(89)90036-4).
- [24] M.H.R. Lankhorst, H.J.M. Bouwmeester, Determination of oxygen nonstoichiometry and diffusivity in mixed conducting oxides by oxygen coulometric titration. II. Oxygen nonstoichiometry and defect model for La_{0.8}Sr_{0.2}CoO_{3-δ}, *J. Electrochem. Soc.* 144 (1997) 1268–1273, <https://doi.org/10.1149/1.1837581>.
- [25] J. Song, S. Zhu, De Ning, H.J.M. Bouwmeester, Defect chemistry and transport properties of perovskite-type oxides La_{1-x}Ca_xFeO_{3-δ}, *J. Mater. Chem. A* 9 (2021) 974–989, <https://doi.org/10.1039/d0ta07508f>.
- [26] A. Maignan, D. Flahaut, S. Hébert, Sign change of the thermoelectric power in LaCoO₃, *Eur. Phys. J. B* 39 (2004) 145–148, <https://doi.org/10.1140/epjb/e2004-00179-8>.